Electronic surface states within a new phase-shift multiple-scattering Green function approach

1991 J. Phys.: Condens. Matter 3 5525

(http://iopscience.iop.org/0953-8984/3/29/007)

J. Phys.: Condens. Matter 3 (1991) 5525–5541. Printed in the UK

Electronic surface states within a new phase-shift multiple-scattering Green function approach

Marian Radny
Institute of Experimental Physics, University of Wrocław, ul. Cybulskiego 36, 50-205 Wrocław, Poland

Received 3 July 1990, in final form 26 February 1991

Abstract. A new phase-shift multiple-scattering approach to the study of the main features of an electron trapped in hydrogenic-like states at solid surfaces (image-induced surface states) is presented. The basic properties of these states are discussed by means of the Green function obtained within the semiclassical path integral method. The Bohr-like quantization condition for the existence of bound surface states was obtained explicitly as poles of the constructed Green function, while the image-induced surface resonances are discussed via the local density of states. Simple calculations of the surface-states binding energy and the local density of states for low-index faces of Al, Au and Cu are also presented.

1. Introduction

In electronic surface physics, fundamental understanding of the clean surface electronic structure is a subject of significant current interest owing to the variety of surface processes that it governs. Within the last decade, owing to the evolution of precise high-resolution angle-resolved photoemission (ARP) [1–3], inverse photoemission (IPS) [4–6] and two-photon photoemission experiments [7], the characterization of electronic surface states existing on nominally clean surfaces has been drastically changed. Apart from the well known intrinsic (Shockley or crystal-induced) surface states, the real, long-range (image) potential outside the solid surface creates a hydrogen-like quantum well in which an electron can be trapped in one of n-numbered Rydberg-like states [8, 9]. These states, usually called image-induced surface states, are properly described by first-principles calculations [10] as well as being reasonably well predicted within the simple phase-shift multiple-reflection theory. This approach, originally developed by Echenique and Pendry [11–13], has been successfully applied by Smith [6, 14–16], Dose [5, 17] and Borstel and Thorner [18], among others, to predict and characterize the uniform picture of the crystal-induced and barrier- (image-) induced surface electronic states in metals. Recently, by constructing the Green function for a quantum well, we have demonstrated for the first time [19] the ability of the extended phase-shift multiple-reflection theory to calculate the local surface density of states for image-induced surface resonances measured in an IPS experiment [20–23]. A question we address in this paper is to what extent the construction of the Green function (or propagator) for the surface quantum well can change the conventional phase-shift accumulation theory of Echenique and Pendry. The motivation for asking this question is twofold. There may be a

0953-8984/91/295525 + 17 $03.50

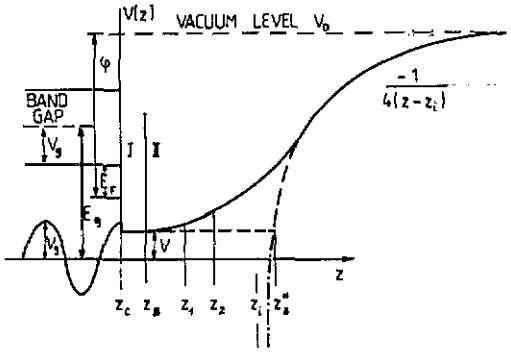

Figure 1. Schematic representation of the expected image-like potential barrier (full curve) compared with the cut-off image potential model (broken curve). The flat potential region for the cut-off barrier extends up to z_B^* (adjustable image plane) while for the smooth potential barrier model ($z_B - z_C$) can be infinitesimally small. The appropriate parameters V_g, E_g, z_i and V_0 are shown.

conceptual advantage to the Echenique and Pendry point of view. On the other hand, there is a practical matter involved in the approach presented here.

The outline of this paper is as follows. In section 3 we present a formal derivation of the fundamental equations. The multiple scattering of the electron is regarded as being made up of a sum over paths of the electron undergoing individual scattering from the separate crystal and surface potentials. Our previous paper [19] outlines the derivation of the local density of states (LDOS) limited to the space between the scatterings where the electron propagates in a way that is independent of these separate potentials. The careful WKB-like (Wentzel–Kramers–Brillouin) analysis performed here provides the Green function determined in any point of the space outside the crystal, i.e. one can calculate the LDOS in the region where the influence of the image potential barrier on the image-induced electron surface states is the most significant. As before, the individual scattering events are completely defined by the magnitude and phase-shift of the surface barrier and crystal reflectances. Furthermore, path integral analysis leads to the new, general formula for the image potential phase change ϕ_B, which to our knowledge has never appeared in the literature before. Finally, for comparison with the simple quantum-mechanical systems, the 'jellium' case is discussed in brief.

Section 4 contains results of numerical calculations. All of them verify directly the usefulness of the phase-shift multiple-scattering Green function method presented in this paper. Namely, the analyses of delocalized states (Al(1 1 1)), image-induced surface resonances (Au(1 1 1)) and image-induced bound surface states (Cu(0 0 1)) are presented via the LDOS calculations. We want to point out that only the last case can be discussed properly within the simple phase model [15]. All calculations have been performed using the Jones, Jennings and Jepsen [24, 25] analytical model for the smooth image potential barrier (figure 1, full curve). For completeness, the phase-shift accumulation theory of Echenique and Pendry will be reviewed below.

2. Background

A crystal is arbitrarily terminated at some plane z_C (figure 1) on which the potential is the same as in the bulk

$$V_C(z) = V_{Cr}(z) + iV_{Ci} \tag{1}$$

where V_{Ci} is a small finite imaginary part accounting for inelastic events.

Outside the adjustable image plane z_B^* the potential is assumed to have an image form, i.e. we will analyse in this section the cut-off image barrier model (figure 1, broken curve)

$$V_B(z) = V_0 - [2(z - z_i)]^{-1} \tag{2}$$

(Rydberg atomic units are used throughout) where z_i and V_0 denote the image plane and the vacuum level, respectively; Im $V_B(z) = 0$ for simplicity and $V_B(z, E) = V_B(\bar{r}, E)$, i.e. the corrugation effects are negligible. For z smaller than z_B^* the z-dependent surface potential is approximated by a constant value $V = V_B(z_B^*)$.

The conventional Echenique and Pendry approach [11] considers the surface states as electron waves trapped between the band-gap region and the surface barrier. In its elementary form [6, 11, 14] if $R_C = r_C e^{i\phi_C}$ and $R_B = r_B e^{i\phi_B}$ represent the respective reflection amplitudes of waves reflected from these barriers, bound surface states exist if

$$r_C = r_B = 1 \tag{3a}$$

and

$$\phi_C + \phi_B + 2k(z_B^* - z_C) = 2n\pi \qquad n = 0, 1, 2, \ldots \tag{3b}$$

where ϕ_B and ϕ_C are the energy-dependent phase changes evaluated at z_B^* and z_C respectively, and k is the perpendicular momentum of the electron wave

$$k = [(E - V) - \bar{k}_\parallel^2]^{1/2}. \tag{4}$$

The index n in equation (3b) denotes the number of extrema in the surface-states wavefunction beyond the outermost atomic layer [8, 26]. At $\bar{\Gamma}$ ($\bar{k}_\parallel = 0$), $n = 0$ solutions designate usual crystal-induced (intrinsic or Shockley) states and $n = 1, 2, \ldots$ solutions constitute the Rydberg series of the image surface states converging to vacuum level V_0.

The Bohr-like quantization condition (3b) requires both the absence of damping processes (Im $V_C = 0$), and that the energies E are in a relative bulk band gap ($r_C = 1$) as well as below the vacuum level ($r_B = 1$). If E extends outside these ranges or inelastic processes are taken into account, the stationary condition (3) must be replaced by the weaker one [18]

$$|1 - r_C r_B \exp\{i[\phi_C + \phi_B + 2k(z_B^* - z_C)]\}|^2 \to \min. \tag{5}$$

The phase changes $\phi_{B(C)}$ produced by any general potential barrier can be obtained by matching both the convergent solution of the Schrödinger equation $\Psi(z)$ and its derivative $\Psi'(z)$ outside and inside the barrier [13, 27]

$$\phi = 2\tan^{-1}[\Psi'(z_0)/k\Psi(z_0)] \tag{6}$$

where z_0 is the coordinate at the boundary barrier and k is defined by equation (4).

The phase-shift ϕ_C imposed in the scattering process on the crystal surface is usually calculated in the simple nearly-free-electron (NFE) approximation [8, 9, 17, 18] (section 4.1). In more realistic models the low-energy electron diffraction (LEED) calculation scheme is used to describe the scattering at the crystal potential [28, 29]. Such calculations yield both r_C and ϕ_C as functions of energy (Im $V_C(z) \neq 0$), so that the non-stationary condition (equation (5)) should be taken into account [18, 28].

The phase-shift ϕ_B occurring on the vacuum side of the surface quantum well depends on the detailed model of the surface potential barrier [24, 25, 28]. Although the long-range part of this barrier is purely electrostatic in nature and decays as $1/2z$ into

the vacuum (equation (2)), ϕ_B should be calculated by numerical integration of the Schrödinger equation along the z axis [15, 16, 28]. However, for the *ad hoc* image potential term introduced into the wave equation (cut-off-image potential—see equation (2) and figure 1), an analytical formula for ϕ_B can be obtained

$$k \tan(\phi_B) = -(\mathrm{d}/\mathrm{d}z)\{\ln[W_{1/2,\alpha}(y)]\}|_{y=y_0} \tag{7}$$

where $W_{1/2,\alpha}(y)$ denotes the Whittaker function, i.e. the convergent solution of the Schrödinger equation inside the barrier; $\alpha = (V_0 - E)^{1/2}$, $y = (z_B^* - z)/\alpha$ and $y_0 = (z_B^* - z_0)/\alpha$.

A useful approximation for ϕ_B was presented by Wannier [30], who approximated the Whittaker solutions by Bessel functions

$$\phi_B = 2 \tan^{-1}\left(\frac{2[J_0(y_0)\cos(\alpha\pi) + Y_0(y_0)\sin(\alpha\pi)]}{ky_0[J_1(y_0)\cos(\alpha\pi) + Y_1(y_0)\sin(\alpha\pi)]}\right) \tag{8}$$

where $J_{0(1)}$ and $Y_{0(1)}$ are the Bessel functions, $y_0 = (4z_i)^{1/2}$, k is given by (4) and α is related to the energy as in equation (7). This approximation is designed to be good at energies far above the cut-off level [13, 26, 31].

The simplest expression for the phase change ϕ_B at the image barrier, namely

$$\phi_B = \{[3.4\ \mathrm{eV}/(V_0 - E)]^{1/2} - 1\}\pi \tag{9}$$

was obtained within the semiclassical approximation by McRae and Kane [32].

Within the last few years, a large experimental database (clean surfaces) has been interpreted with the use of the phase accumulation model. Although this model accounts successfully for the systematics of bound image surface states, it fails in the case of image-induced surface resonances [15, 23]. On the other hand, the same simple phase model has been found to work well in the case of O and Na chemisorbed on low-index copper faces [16, 33].

3. Analysis

The path-integral-inspired semiclassical method has given a new approach to the construction of the Green function and thus the approximate quantum-mechanical description of simple quantum systems [34]. The usefulness of this method [35] has been proved by a detailed investigation of the single quantum well including both discrete and continuum states [36, 37]. Recently, we have presented simple calculations performed by means of this method considering the effect of the image potential barrier on the local density of states at metal surfaces [19]. Of interest here is to generalize the previously obtained results by a careful study of the Green function for any smooth image-like potential outside the crystal surface (figure 1, full curve). For the quantitative analysis performed in section 4, we adopt the analytical barrier model proposed by Jones, Jennings and Jepsen (JJJ) [24, 25].

3.1. Green function for surface quantum well

In general, the fixed energy Green function in the position representation for a one-electron Hamiltonian H is

$$G(z_1, z_2, \bar{k}_\parallel = 0; E) = \mathrm{i}\langle z_1|(E - H)^{-1}|z_2\rangle/2\pi \tag{10}$$

for z_1, z_2 inside the well (figure 1), and $H = T + V_S$, where T is the kinetic energy and V_S the potential energy operator of the system.

The idea is that the propagator (10) can be expressed as a sum over paths that connect the points z_1 and z_2 [34, 36]

$$G(z_1, z_2, \bar{k}_\parallel = 0; E) = \{(i/2\pi)[K(z_1)K(z_2)]^{-1/2}\} \sum_{\text{paths}} \prod f_m \tag{11}$$

where $K(z)$ is the local wavenumber defined by

$$K(z) = \begin{cases} k = (E - V)^{1/2} & z_C < z < z_B \quad (12a) \\ k(z) = [E - V_B(z)]^{1/2} & z_B < z. \quad (12b) \end{cases}$$

Here $V = V_B(z_B)$ in equation (12*a*) and $V_B(z)$ in (12*b*) represents any smooth image-like potential outside the infinitesimally flat potential region ($z_B - z_C$) (figure 1, full curve).

The sum in equation (11) is over *all* topologically distinct paths between z_1 and z_2 inside the well, while f_m are the amplitude phase factors associated with the segments of each path

$$f_m = \exp\left(i \int_{z_1}^{z_2} K(z)\, dz\right). \tag{13}$$

Let us imagine the particle wave incident on the wells inside the surface quantum well with energy $V < E < V_0$. For the points z_1, z_2 where $z_C < z_1 < z_2 < \infty$, we have two classical turning points, namely

(i) on the crystal–vacuum interface at $z = z_C$, and
(ii) on a finite surface barrier at $z = b$ defined by $V_B(b) = E$.

The reflectance of the electron wave from the boundary that we fixed to be our coordinate origin (z_C) is $R_C = r_C e^{i\varphi_C}$. Consider now the case of reflection of the electron wave from the surface barrier. Let us assume that the condition on the total reflectivity is fulfilled ($r_B = 1$). In the region $z > z_B$ to the turning point b ($V_B(b) = E$), the phase of the reflected wave is accumulated from the segments of each path according to equation (13). For the points z_1, z_2, which are in region II in figure 1, we need the propagator $G(z_1, z_2, \bar{k}_\parallel = 0; E)$ where

$$z_1, z_2 < b \tag{14}$$

and the different paths by which travel from z_1 to z_2 can be characterized as follows:

(i) Propagate along the direct path from z_1 to z_2 ($n = 0$); propagate from z_1 to the turning point b, then to the turning point z_C, and back to z_2 ($n = 1$), etc. Summing up all the possible ways without leaving the well one can easily obtain the whole amplitude in this case, namely

$$\exp\left(i \int_{z_1}^{z_2} k(z)\, dz\right) \sum_{n=0}^{\infty} \left\{(R_C r_B)^n \exp\left[2ni\left(k(z_B - z_C) + \int_{z_B}^{b} k(z)\, dz\right)\right]\right\}. \tag{15a}$$

(ii) Propagate from z_1 to the turning point z_C, then back to z_2 ($n = 0$); propagate

from z_1 to the turning point z_C, then to the turning point b, then again to turning point z_C, and then back to z_2 ($n = 1$), etc. In this case

$$R_C \exp[i2k(z_B - z_C)] \exp\left(2i\int_{z_B}^{z_1} k(z)\,dz\right) \exp\left(i\int_{z_1}^{z_2} k(z)\,dz\right)$$
$$\times \sum_{n=0}^{\infty} \left\{(R_C r_B)^n \exp\left[2ni\left(k(z_B - z_C) + \int_{z_B}^{b} k(z)\,dz\right)\right]\right\}. \tag{15b}$$

(iii) Propagate from z_1 to the turning point z_C, next to the turning point b, and then back to z_2 ($n = 0$), etc. Then

$$R_C r_B \exp[i2k(z_B - z_C)] \exp\left(2i\int_{z_B}^{b} k(z)\,dz\right) \exp\left(i\int_{z_2}^{z_1} k(z)\,dz\right)$$
$$\times \sum_{n=0}^{\infty} \left\{(R_C r_B)^n \exp\left[2ni\left(k(z_B - z_C) + \int_{z_B}^{b} k(z)\,dz\right)\right]\right\}. \tag{15c}$$

(iv) Propagate from z_1 to the turning point b and then back to z_2 ($n = 0$); propagate from z_1 to the turning point b, then to the turning point z_C, then to the turning point b, and then back to z_2 ($n = 1$), etc. Then

$$r_B \exp\left(2i\int_{z_B}^{b} k(z)\,dz\right) \exp\left(-2i\int_{z_B}^{z_1} k(z)\,dz\right) \exp\left(i\int_{z_2}^{z_1} k(z)\,dz\right)$$
$$\times \sum_{n=0}^{\infty} \left\{(R_C r_B)^n \exp\left[2ni\left(k(z_B - z_C) + \int_{z_B}^{b} k(z)\,dz\right)\right]\right\}. \tag{15d}$$

Now, according to equation (11) the semiclassical approximation to the full propagator is given by the sum over all paths (15*a–d*), and

$$G(z_1, z_2, \bar{k}_{\parallel} = 0; E) = \{(i/2\pi)[k(z_1)k(z_2)]^{-1/2}\}\left\{\exp\left(i\int_{z_1}^{z_2} k(z)\,dz\right)\right.$$
$$+ \exp\left[i\left(k(z_B - z_C) + \int_{z_B}^{b} k(z)\,dz\right)\right](R_C e^{iT} + r_B e^{-iT})$$
$$\left. + R_C r_B \exp\left[i\left(2k(z_B - z_C) + \int_{z_B}^{b} k(z)\,dz\right)\right] \exp\left(i\int_{z_2}^{z_1} k(z)\,dz\right)\right\}$$
$$\times \left\{1 - R_C r_B \exp\left[2i\left(k(z_B - z_C) + \int_{z_B}^{b} k(z)\,dz\right)\right]\right\}^{-1} \tag{16a}$$

where

$$T = k(z_B - z_C) - \int_{z_B}^{b} k(z)\,dz + 2\int_{z_B}^{z_1} k(z)\,dz + \int_{z_1}^{z_2} k(z)\,dz. \tag{16b}$$

The above procedure can easily be extended to the case where both the points z_1, z_2 are in region I, i.e. $z_C < z_1 < z_2 < z_B$, and the result is

$$G(z_1, z_2, \bar{k}_\parallel = 0; E) = [\mathrm{i}/(2\pi k)] \left\{ \exp(\mathrm{i}k(z_2 - z_1)) \right.$$
$$+ \exp\left[\mathrm{i}\left(k(z_B - z_C) + \int_{z_B}^{b} k(z)\,\mathrm{d}z\right)\right](R_C\,\mathrm{e}^{\mathrm{i}W} + r_B\,\mathrm{e}^{\mathrm{i}W})$$
$$\left. + R_C r_B \exp\left[\mathrm{i}\left(2k(z_B - z_C) + 2\int_{z_B}^{b} k(z)\,\mathrm{d}z\right)\right] \exp[\mathrm{i}k(z_1 - z_2)] \right\}$$
$$\times \left\{1 - R_C r_B \exp\left[2\mathrm{i}\left(k(z_B - z_C) + \int_{z_B}^{b} k(z)\,\mathrm{d}z\right)\right]\right\}^{-1} \qquad (17a)$$

where

$$W = k[z_1 + z_2 - (z_B + z_C)] - \int_{z_B}^{b} k(z)\,\mathrm{d}z. \qquad (17b)$$

In all equations (15*a–d*), (16*a*, *b*) and (17*a*, *b*), k and $k(z)$ are defined by relations (4), (12*a*) and (12*b*) for region I and II in figure 1, respectively. The parameter R_C denotes the reflectance from the crystal barrier and r_B is the reflectivity from the surface barrier with the appropriate phase change ϕ_B that we want to find.

3.2. Bound surface states and barrier phase change ϕ_B

The electronic surface states localized at the metal surface represent the discrete energy spectrum. The Green function formalism allows one to determine this spectrum as the poles of the appropriate propagator $G(z_1, z_2; E)$ [38]. Thus, according to equations (16*a*, *b*) and (17*a*, *b*) the condition for the existence of the bound surface states is the following:

$$1 - R_C r_B \exp\left[\mathrm{i}\left(2k(z_B - z_C) + 2\int_{z_B}^{b} k(z)\,\mathrm{d}z\right)\right] = 0. \qquad (18)$$

For energies E in the bulk band gap below the vacuum level V_0 (assuming that Im $V_C(z) = 0$)

$$|R_C| = r_C = |R_B| = r_B = 1 \qquad (19a)$$

and equation (18) can be written in the form

$$\phi_C + \phi_B(E) + 2k(z_B - z_C) = 2n\pi \qquad n = 0, 1, 2, \ldots \qquad (19b)$$

where R_C in equation (18) was replaced by $r_C\,\mathrm{e}^{\mathrm{i}\phi_C}$ and $\phi_B(E)$ in equation (19*b*) is defined as

$$\phi_B(E) = 2\int_{z_B}^{b} k(z)\,\mathrm{d}z \qquad (19c)$$

for $k(z)$ from equation (12*b*) and b determined from

$$V_B(b) = E. \qquad (19d)$$

The Bohr-like quantization stationary condition (equation (19*b*)) is the same as the

one derived by Echenique and Pendry in their 1978 paper [11]. The only difference is due to the energy-dependent barrier phase change ϕ_B in equation (19*c*).

What energy dependence of ϕ_B can be expected?

Following equations (2) and (12*b*), i.e. taking into account the simple cut-off surface barrier model from figure 1 (broken curve), the analytical formula for ϕ_B can be written as

$$\phi_B(E) = -\tfrac{1}{2}[(E-V)^{1/2}/2(V_0-V)] + [2(V_0-E)^{1/2}]^{-1}\tan^{-1}\{[(E-V)/(V_0-E)]\} \qquad (20)$$

where, because of (19*d*) and $V_B(z_B^*) = V$ the parameters b and z_B^* in the integral (19*c*) were written in the form

$$b = z_i + [2(V_0 - E)]^{-1} \qquad (21a)$$

$$z_B^* = z_i + [2(V_0 - V)]^{-1}. \qquad (21b)$$

Note that, as the energy approaches the vacuum level V_0, the variation of ϕ_B (equation (20)) becomes infinitely rapid and according to equation (19*b*) the Rydberg series of image states is generated. We want to point out that such energy dependence of ϕ_B is characteristic for any image-like surface potential barrier (section 2, equations (6)–(9) and section 4, figure 4). At the bottom of the continuum, where the wave incident on the surface has zero energy, the surface potential barrier (independent of its shape) behaves like an infinite barrier. Hence, from equation (6) for a step potential barrier we obtain $\phi_B = -\pi$ ($E \to 0$) and finally

$$\phi_B(E) = 2\int_{z_B}^{b} k(z)\,\mathrm{d}z - \pi. \qquad (22)$$

To our knowledge, formula (22) has never appeared in the literature before. Within the semiclassical approach, this expression is as general as the one obtained from the quantum-mechanical analysis (equation (6)). The quantitative aspect of this relation will be discussed in section 4.

3.3. Local density of states

Excited electrons are subjected to inelastic electron–electron interactions, which results in decay processes, i.e. broadening of true (bound) surface states to resonances. The existence of the resonances is not associated with the singularity of the appropriate Green function. In this case a quantity of considerable physical interest is the density of states determined by the imaginary part of the propagator. For $z = z_1 = z_2$ the local density of states (LDOS) is defined as [38]

$$n_{\bar{k}_\parallel=0}(z, E) = -\mathrm{Im}[\langle z|(E-H)^{-1}|z\rangle]/\pi. \qquad (23)$$

Following equations (16), (17) and (19*c*) the expression for the LDOS in our system is

$$n_{\bar{k}_\parallel=0}(z; E) = [1/2\pi^2 k(z)]\left[1 - (r_B r_C)^2 + r_C(1 - r_B^2)\right.$$

$$\left.\times \cos\left(2k(z_B - z_C) + \phi_C + 2\int_{z_B}^{z} k(z')\,\mathrm{d}z'\right)\right.$$

$$+ r_B(1 - r_C^2)\cos\left(\phi_B - 2\int_{z_B}^{z} k(z')\,dz'\right)\Big]$$

$$\times |1 - r_C r_B \exp\{i[2k(z_B - z_C) + \phi_B + \phi_C]\}|^{-2} \tag{24}$$

for $z_B < z < \infty$ in region II, and

$$n_{\bar{k}_\parallel=0}(z; E) = (1/2\pi^2 k)\{1 - (r_C r_B)^2 + r_C(1 - r_B^2)\cos[2k(z - z_C) + \phi_C]$$
$$+ r_B(1 - r_C^2)\cos[2k(z - z_B) - \phi_B]\}|1 - r_C r_B$$
$$\times \exp\{i[2k(z_B - z_C) + \phi_B + \phi_C]\}|^{-2} \tag{25}$$

for $z_C < z < z_B$ in region I (figure 1).

We want to point out that equation (25) appears to be a special case of expression (24) ($k(z) = \text{const}$) and in this form was presented in our previous work [19].

3.4. Jellium case

The solution of the Schrödinger equation in the free-electron model of solid surfaces (simple metals) is given by the combination of the plane waves inside the bulk which matches onto the solution in vacuum and the surface region. The local density of states in this case is simplified to [39]

$$n(z; E) = (1/\pi k)\{1 + \cos[2kz - \kappa(E)]\} \tag{26}$$

where $k = E^{1/2}$. The function $\kappa(E)$ is the phase-shift, i.e. the incident wave $\exp(i\bar{k}_\parallel \bar{r}_\parallel)\exp(-ik_z z)$ from the bulk is reflected by the surface with a phase-shift 2κ. For the image potential (figure 1), $\kappa = \phi_B$, where ϕ_B is given by equations (6)–(9), (20) or (22).

In the phase-shift Green function approach presented here, the 'jellium' case could be obtained by putting $r_C = 0$ in equations (24) and (25), so that

$$n_{k_\parallel=0}(z; E) = (1/2\pi^2 k)\{1 + r_B\cos[2k(z - z_B) - \phi_B]\} \tag{27}$$

for $z < z_B$, and

$$n_{k_\parallel=0}(z; E) = [1/2\pi^2 k(z)]\left[1 + r_B\cos\left(\phi_B - 2\int_{z_B}^{z} k(z')\,dz'\right)\right] \tag{28}$$

for $z > z_B$, where k and $k(z)$ are given by equation (12).

Equations (26) and (27) are identical ($r_B = 1$). In both cases, the first term gives the bulk density of states, and the second the interference effects due to the surface. Since, in general, the image potential leads to barrier phase changes $\phi_B(E)$ as in equation (9) (see also section 3.2, equation (20)), $n(z; E)$ oscillates as we move up to the vacuum level V_0 (see section 4.3).

The local density of states for the non-constant potential region (vacuum side in figure 1) is described here by equation (28). For $k(z) = \text{const}$, equations (27) and (28) are the same, so the formula (27) as well as (17) and (25) represent exact solutions.

3.5. Inelastic and diffraction effects

Lifetimes of individual electrons have usually been connected with peak widths in the ARP and IPS spectra from solid surfaces [40, 41]. Theoretically, in the one-electron

picture, the absorption effects can be described by means of an optical potential (Im $V_C \neq 0$) [42]. Namely, the one-electron Green function reads simply as

$$G(E) = (E - T - V_S)^{-1} = (E - iV_{Ci} - T - V_{Cr} - V_B)^{-1}. \tag{29}$$

Thus introduction of the imaginary component of V_C is equivalent to replacing E by $E - iV_{Ci}$ in the Green function for undamped system ($V_{Ci} = 0$). This means that all the singularities representing a single-particle excitation are moved off the real energy axis into the complex energy plane by an amount V_{Ci}, with the corresponding broadening of the electron states, i.e. δ-functions become Lorentzian peaks with finite width at half-maximum.

If we include the inelastic processes as an imaginary component iV_{Ci} to E, the expression for ϕ_C in the multiple-scattering approach is

$$\exp[i\phi_C(E + iV_{Ci})] = \exp\{i[\phi_C(E) + iV_{Ci}(\partial\phi_C/\partial E)]\} \tag{30}$$

where a linear approximation to the complex energy dependence of the phase has been made [11].

On the other hand, the diffraction effects reduce r_C to less than unity even in the case of the absence of absorption caused by inelastic processes (Im $V_C = 0$). In the energy region outside the energy gap [29]

$$r_C = \{[ik\psi(z_C) + \psi'(z_C)]/[ik\psi(z_C) - \psi'(z_C)]\}\, e^{-i2kz_C} < 1 \tag{31}$$

where ψ represents the crystal wavefunction and the prime marks differentiation. In this case the imaginary part of the crystal phase change is

$$r_C\, e^{i\phi_C} = \exp\{i[\phi_C + i\ln(r_C)]\}. \tag{32}$$

Incorporating both these processes as the imaginary component to the crystal phase change we can write [11]

$$r_C \exp[i\phi_C(E + iV_{Ci})] = \exp\{i[\phi_C + i\ln(r_C) + iV_{Ci}(\partial\phi_C/\partial E)]\}. \tag{33}$$

The usefulness of this relation in our discussion concerning the image-induced surface states will be presented in section 4.

4. Numerical results

The aim of this part of our paper is to explore what the local density of states (LDOS) analysis can tell us about changes in the surface electronic structure due to the surface barrier shape and crystal band structure.

In general, the hydrogen-like image-induced surface states, if they exist, are pinned to the vacuum level V_0 (upper limit). As follows from the analysis in sections 3.2–3.4, the basic properties of these states should depend strongly on the value of the crystal reflectivity r_C and, consequently, on the energy position of the vacuum level V_0 relevant

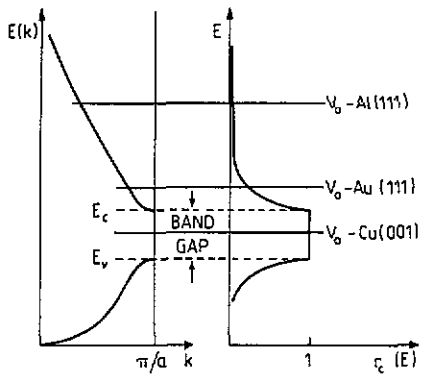

Figure 2. Schematic representation of the dispersion relation $E(k)$ and energy variation of the crystal reflectivity $r_C(E)$ for the simple two-band nearly-free-electron model. The vacuum level position (V_0) relevant to the band gap is schematically indicated for three different cases—see the text.

to the band gap. In figure 2 three especially interesting cases are indicated: Al(1 1 1) (delocalized states), Au(1 1 1) (image-induced surface resonances) and Cu(0 0 1) (image-induced bound surface states). The quantitative analysis presented in sections 4.3, 4.4 and 4.5 has been performed with the use of the canonical formulae of the phase-shift Green function approach: (24) and (25), together with (27), (28) and (32). To use them the parameters (ϕ_C, r_C) (section 4.1) and (ϕ_B, r_B) (section 4.2) have to be determined.

4.1. Crystal phase changes ϕ_C

We are interested in the bulk L gap for the (1 1 1) and the bulk X gap for the (0 0 1) faces of the FCC crystal. The model potential we adopt in our calculations is of a real band structure to represent the solid side (Im $V_C = 0$). We consider the gap to be NFE-like opened by potential Fourier components V_g corresponding to the lattice vector g normal to the surface that we study (two-band model). The four parameters needed for calculation, namely V_g, E_g, the Fermi level E_F and the workfunction φ, are represented in figure 1. V_g is taken as half the width of the gap that we are considering and E_g ($=g^2/8$) is the energy difference between the centre of the gap and the crystal inner potential.

According to (6) and following Smith [14], ϕ_C in the energy gap can be found ($r_C = 1$),

$$k \tan(\phi_C/2) = (g/2) \tan(\pi/2 + \delta) - q \tag{34}$$

where k is determined in equation (12a) and δ denotes the phase of the wavefunction inside the crystal $z < z_C$,

$$\sin(2\delta) = -qg/2V_g \tag{35}$$

and

$$q^2 = -2(E + E_g) + 2(4EE_g + V_g^2). \tag{36}$$

Outside the band gap $\phi_C = \text{const}$ while r_C decreases rapidly ($r_C < 1$, equation (31)). This situation is illustrated schematically in figure 2 for the simple two-band NFE model. Inside the energy gap $r_C = 1$ and $\phi_C(E)$ changes from 0 to π (equation (34) and curve 1 in figure 4).

4.2. Surface barrier shape

The barrier phase change $\phi_B(E)$ ($r_B = 1$) was determined from equations (22) and (12*b*) for the analytical surface barrier model proposed by Jones, Jennings and Jepsen (JJJ) [24, 25] as well as for the cut-off image potential (figure 1, broken curve, and equation (2)).

(i) The surface barrier shape in the JJJ model is approximated by

$$V_B(z) = \begin{cases} V_0 - [2(z - z_i)]^{-1}\{1 - \exp[-\lambda(z - z_i)]\} & z > z_i \\ V_0 - U_0\{A \exp[B(z - z_i) + 1]\}^{-1} & z < z_i. \end{cases} \tag{37}$$

It has an asymptotic form similar to the shifted image potential with a smooth transition to its bulk value U_0 (z_i denotes the image plane and λ is the characteristic distance over which the image potential saturated to the Fourier transform of the bulk potential). The values of these three adjustable parameters for different surfaces of Al, Ni, Cu, Au, ... was determined in [25] by fitting the effective surface potential from first-principles self-consistent slab calculations to the model potential of equation (37). The parameters A and B are fixed by the requirement of smooth continuity at $z = z_i$ so $B = U_0/A$ and $A = -1 + 2U_0/\lambda$.

(ii) Two arbitrary parameters in the cut-off model potential (figure 1, broken curve, and equation (2)) are the depth of the flat potential region V and the image plane z_i (or the distance between the image plane z_i and the surface z_C—the crystal terminates at half an interlayer spacing outside the topmost atomic layer). In general the flat potential is matched into the inner potential modulated by the V_g and the choice of V would be equally physically justified for any value in the range $\pm|V_g|$. Usually $V = -|V_g| = V_B(z_B^*)$ while z_i is chosen in such a way that the Shockley surface state (crystal-induced; $n = 0$ in equation (3) or (19*b*)) is reproduced in the band gap. For Al(1 1 1) $V_g = 0.01764$ Ryd (lattice constant $a = 7.655$ au and $V_0 = 15.21$ eV), so that $z_i = 1.2$ au (see the next section, figures 3(*b*) and 4).

4.3. Al(1 1 1)—delocalized states

The effect of the image potential barrier on the local density of states (LDOS) is evident in the calculations presented in figure 3(*a*) and performed for the 'jellium' model ($r_C = 0$, section 3.4) and the JJJ surface barrier. As can be seen from equations (27), (28), (9) and (20) the oscillations on each LDOS curve in figure 3(*a*) arise due to the barrier phase change ϕ_B. In figure 4 we present two $\phi_B(E)$ curves calculated for the cut-off image potential barrier (equation (2)) using two different expressions: the exact one given by equation (7) (curve 2) and relation (22) derived from the extended phase-shift method (curve 3). As can be seen, the differences are not significant and $\phi_B(E) \to \infty$ for $E \to V_0$. The adjustable parameter for the cut-off image potential is the image plane and for $z_i = 1.2$ au the Shockley surface state is reproduced in the band gap for both curves 2 and 3—dots in the inset in figure 4.

For the JJJ barrier (37) with $\lambda = 1.0$ au, $V_0 = 1.08$ Ryd and $z_i = 2.95$ au (parameters appropriate for Al(1 1 1) [25] which were used for calculations presented in figures 3(*a*), (*b*)), the $\phi_B(E)$ dependence represented by curve 4 in figure 4 is qualitatively the same as for the cut-off surface barrier. The appreciable quantitative differences between curves 2 (3) and 4 reflect the fact that ϕ_B changes less rapidly for smooth potential barriers.

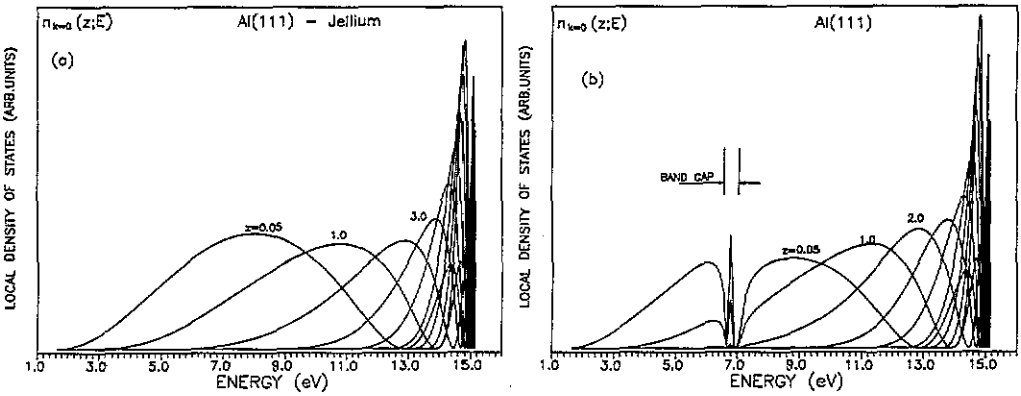

Figure 3. Al(1 1 1). The local density of states $n_{k_{\parallel}=0}(z; E)$ calculated for $z = 0.05$, 1.0, 2.0, 3.0, 4.0, 5.0, 6.0, 7.0 and 8.0 au and the JJJ barrier model: (*a*) $r_C(E) = 0$, jellium case; (*b*) $r_C(E) \neq 0$ (equation (31)). Inside the band gap $r_C = 0.97$ and the peak denotes the Shockley ($n = 0$) surface state.

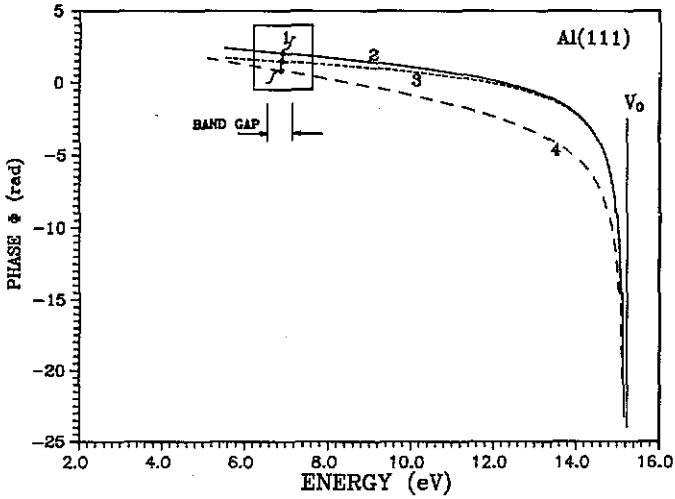

Figure 4. Energy variation of the cut-off image potential phase-shift ($-\phi_B$) as given by equations (7) (curve 2), and (20) (curve 3). Curve (4) corresponds to $-\phi_B$ calculated for the JJJ barrier from equation (22). In the inset the crystal phase change (ϕ_C) in the band gap is presented (curve 1). Dots represent the graphical solution of the Bohr-like quantization condition for $n = 0$ (Shockley state). Parameters appropriate for Al(1 1 1).

Figure 3(*b*) shows the local density of states at the Al(1 1 1) surface when the proper $r_C(E)$ ($\neq 0$) dependence (31) is taken into account. It is interesting to see how the energy band structure of Al is created with a sharp peak in the band gap. This peak represents the Shockley (crystal-induced) surface state. It is related to a dot on curve 4 in the inset in figure 4, where graphical solutions of the Bohr-like quantization condition (19*b*) for $n = 0$ are presented. We want to point out the adequacy of the JJJ barrier parameters for the crystal surface states calculation, i.e. in contrast to the cut-off potential the Shockley surface state is reproduced here without any adjustable parameters. Outside the gap we

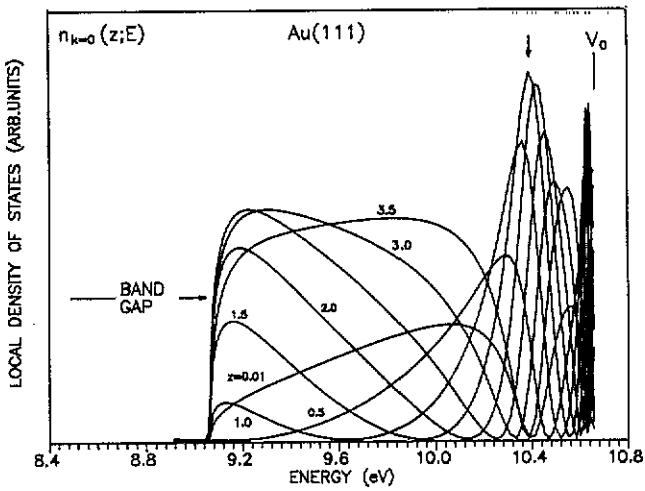

Figure 5. Au(1 1 1). The local density of states $n_{k_\parallel=0}(z;E)$ calculated at $z = 0.01, 0.5, 1.0, 1.5, 2.0, 2.5, 3.0$ and 3.5 au. The arrow at ~0.29 eV below the vacuum level V_0 indicates the image-induced resonant state.

again see that $n_{k_\parallel=0}(z;E)$ oscillates in the same way as in the 'jellium' model in figure 3(*a*). We conclude that the value of $r_C(E)$ just below the vacuum level ($\sim 10^{-2}$ in this case) acts as a relatively weak perturbation in equations (24) and (25), so that the LDOS picture in figure 3(*a*) as well as figure 3(*b*) represents the density of *delocalized* states. Other investigations confirm this result [43–45]. On the other hand, however, the experimental observation of the image-induced surface resonant state at Al(1 1 1) has been reported in the literature [21].

4.4. Au(1 1 1)—image-induced surface resonances

The LDOS analysis for Au(1 1 1) has been performed for the JJJ barrier model (λ = 1.25 au, $V_0 = 0.9609$ Ryd, $z_i = 2.41$ au) [25] and the two-band NFE approximation (V_g = 0.169 Ryd, $a = 7.72$ au, $V_0 = 0.7915$ Ryd) [23]. The results of the calculations are presented in figure 5. An important and interesting difference between the results in figures 3(*a*, *b*) for Al and figure 5 is that one can see how different LDOS build up the image-induced resonant state outside the band gap at ~0.29 eV below the vacuum level V_0. It is clear from equation (24) and the analysis in section 3.4 that such oscillations in $n_{k=0}(z;E)$ as shown in figure 5 are caused by the interference between the incident and partially reflected ($r_C \sim 10^{-1}$) waves inside the surface quantum well.

It is also interesting to compare the position of the image resonant state roughly estimated above to the results obtained from the simple phase accumulation model: −0.85 below V_0 [23]. Since the measured value of this energy position is ~0.42 eV below V_0 the authors conclude (see also [15]) that the elementary phase model (equation (5)) is not applicable for the image-induced resonant states analysis. It looks like the phase-shift Green function approach offers a qualitatively new result.

4.5. Cu(0 0 1)—image-induced bound surface states

Now we move on to the energy band gap where the crystal reflectivity $r_C = 1$ (figure 2 and equation (31)) and instead of the relation (24) for LDOS the Bohr-like quantization

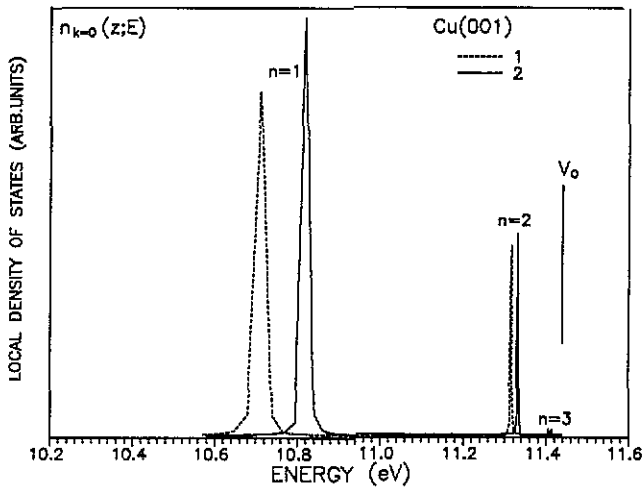

Figure 6. Cu(0 0 1). The local density of states $n_{k_\parallel=0}(z;E)$ calculated in the energy gap for $r_C = 0.98$, $z = 0.4$ au and two sets of JJJ parameters: (1) $\lambda = 1.15$ au, $V_0 = 1.12$ Ryd, $z_i = 2.40$ au; (2) $\lambda = 1.05$ au, $V_0 = 0.85$ Ryd, $z_i = 2.35$ au. The bound image surface states are denoted $n = 1, 2, 3, \ldots$.

condition (equations (3*b*) and (19*b*)) should be used. In general, however, when the electron encounters a band gap instead of an infinite barrier, its wavefunction penetrates into the crystal. The overlap of the image state wavefunction with the crystal tells us how much effects associated with elastic and inelastic scattering inside the crystal affect the electron in the image state. Therefore, these effects are important in determining the lifetime of this state. According to equations (30)–(33) we can make these ideas a little more quantitative but still remain within a simple intuitive approach. Namely, as was pointed out in section 3.5, the imaginary part of ϕ_C takes its origin from the optical potential (Im $V_C \neq 0$) and/or diffraction effects ($r_C < 1$). Formally, each of these terms can be replaced by the other, giving qualitatively the same effect, i.e. the δ-function (bound state) becomes the Lorentzian peak (resonance). The effects of this simulation ($r_C = 0.97$) with the use of equations (22) and (24) are presented in figure 6 for Cu(0 0 1) (two-band model: $V_g = 0.2216$ Ryd, $V_0 = 0.8474$ Ryd, $a = 6.824$ au). Because the determination of the surface barrier shape is not unique [15, 25], the calculations have been performed for two sets of JJJ barrier parameters [25]: $\lambda = 1.15$ au, $V_0 = 1.12$ Ryd, $z_i = 2.40$ au (full curve in figure 6), and $\lambda = 1.05$ au, $V_0 = 0.85$ Ryd, $z_i = 2.35$ au (broken curve). Peaks on each curve represent the image-induced bound surface states, which create the Rydberg-like series of image states. These results also show the sensitivity of the expression (22) to the more or less smooth surface barrier model chosen for calculations.

5. Summary

In this paper we have given a general viewpoint and have examined the general properties of the new phase-shift multiple-scattering Green function approach for the calculation of surface electronic states.

The simple criterion for bound surface state energy (known from the Echenique and Pendry theory)—equations (3) and (19*b*)—as well as the analytical formula for the local density of states—equations (24) and (25)—have canonical form, i.e. detailed information on the surface potential barrier and the crystal have been summarized in the (ϕ_B, r_B) and (ϕ_C, r_C) parameters, respectively. In other words, one need not repeat the whole calculations presented in section 3. All that is necessary is to modify the calculations of (ϕ_B, r_B) and (ϕ_C, r_C) according to the chosen model for the surface potential barrier and the crystal band structure.

We have also shown the usefulness of the new WKB-like formula for determining the barrier phase change ϕ_B. Because of the extreme simplicity of this expression, we recommend further investigations within this context for any smooth image-like potential barriers.

Finally, we want to recommend the extended phase-shift multiple-scattering Green function theory presented here as a powerful method suitable for treating the electronic surface states, overlayer states, lifetime effects, density of states, tunnelling phenomena, etc, in simple qualitative as well as advanced quantitative theoretical electronic surface structure calculations.

References

[1] Feuerbacher B, Fitton B and Willis R F 1978 *Photoemission and Electronic Structure of Surfaces* (Berlin: Springer)
[2] Himpsel F J 1983 *Adv. Phys.* **32** 1
[3] Courths R and Hufner S 1984 *Phys. Rep.* **112** 53
[4] Himpsel F J 1986 *Comments Condens. Matter Phys.* **12** 199
[5] Dose V 1987 *J. Vac. Sci. Technol.* A **5** 2032
[6] Smith N V 1988 *Rep. Prog. Phys.* **51** 1227
[7] Steinmann W 1989 *Appl. Phys.* A **49** 345
[8] Weinert M, Hulbert S L and Johnson P D 1985 *Phys. Rev. Lett.* **55** 2055
[9] Goldman A, Dose V and Borstel G 1985 *Phys. Rev.* B **32** 1973
[10] Hulbert L, Johnson P D and Weinert M 1986 *Phys. Rev.* B **34** 3670
[11] Echenique P M and Pendry J B 1978 *J. Phys. C: Solid State Phys.* **11** 2065
[12] Echenique P M and Pendry J B 1990 *Prog. Surf. Sci.* **32** 111
[13] Ortuno M and Echenique P M 1986 *Phys. Rev.* B **34** 5199
[14] Smith N V 1985 *Phys. Rev.* B **32** 3549
[15] Smith N V, Chen T C and Weinert M 1989 *Phys. Rev.* B **40** 7565
[16] Chen T C and Smith N V 1989 *Phys. Rev.* B **40** 7487
[17] Dose V 1985 *Surf. Sci. Rep.* **5** 337
[18] Borstel G and Thorner G 1987 *Surf. Sci. Rep.* **8** 1
[19] Radny M 1990 *J. Phys.: Condens. Matter* **2** 4661
[20] Kubiak G 1988 *Surf. Sci.* **201** L475
[21] Heskett D, Frank K-H, Horn K, Koch E, Freund H J, Baddorf A, Tseui K D and Plumer E W 1988 *Phys. Rev.* B **37** 10387
[22] Straub D and Himpsel F J 1986 *Phys. Rev.* B **33** 2256
[23] Woodruff D R, Royer W A and Smith N V 1986 *Phys. Rev.* B **34** 764
[24] Jones R O, Jennings P J and Jepsen O 1984 *Phys. Rev.* B **29** 6474
[25] Jones R O, Jennings P J and Weinert M 1989 *Phys. Rev.* B **34** 5199
[26] Stęślicka M, Radny M, Perkal Z and Jurczyszyn L 1987 *Solid State Commun.* **61** 681
[27] Echenique P M 1987 *Am. J. Phys.* **55** 278
[28] Schuppler S, Fischer N, Steinmann W, Schneider P and Bertel E 1990 *Phys. Rev.* **42** 9403
[29] Inglesfield J E and Benesh G A 1988 *Phys. Rev.* B **37** 6682
[30] Wannier G H 1943 *Phys. Rev.* **64** 358
[31] Garcia N and Solana T 1973 *Surf. Sci.* **36** 262

[32] McRae F G and Kane M L 1981 *Surf. Sci.* **108** 435
[33] Lindgren S A and Wallden L 1989 *Surf. Sci.* **211/212** 394
[34] Holstein B R 1983 *Am. J. Phys.* **51** 897
[35] Schulman L S 1981 *Techniques and Applications of Path Integration* (New York: Wiley) ch 2
[36] Trott M and Schnittler Ch 1988 *Phys. Status Solidi* b **152** 153
[37] Radny M unpublished
[38] Economou E N 1983 *Green's Function in Quantum Physics* (Berlin: Springer) ch 3
[39] Inglesfied J E and Holland B W 1981 *The Chemical Physics of Solid Surfaces and Heterogeneous Catalysis* ed D A Kind and D P Woodruff (New York: Elsevier) p 264
[40] Schoenlien R W, Fujimoto F J, Eesley G L and Capehart T W 1988 *Phys. Rev. Lett.* **61** 2596
[41] Nielsen H B, Brostrom G and Matthias E 1989 *Z. Phys.* B **77** 91
[42] Dederics R H 1972 *Solid State Phys.* **27** 136
[43] Radny M 1991 *Surf. Sci.* **247** 143
[44] Lindgren S A and Wallden L 1989 *Phys. Rev.* B **40** 11546
[45] Papadia S, Person W R and Salmi L A 1990 *Phys. Rev.* B **41** 10237